

OZONE BOX MODEL

EVAN WELLMEYER

Professor Giovanni Pitari

Department of Atmospheric Science and Technology

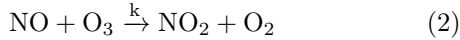
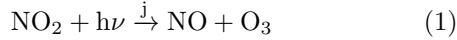
Università Degli Studi Dell'Aquila, L'Aquila

Sapienza Università Di Roma, Rome

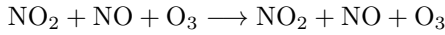
Fall 2021

1 Introduction

Many processes govern ozone concentrations in the PBL. Ozone (O_3) in the troposphere and planetary boundary layer (PBL) is attributed mainly to production via the cycling of nitrogen oxides (NO_x) in the troposphere [1], as well as vertical mixing between the troposphere and the stratosphere, where ozone is formed via UV interaction. NO_x is released through combustion mainly as NO; however, cycling between NO and NO_2 in the PBL takes place during daytime hours on a timescale of minutes [1] via the following catalytic cycle:



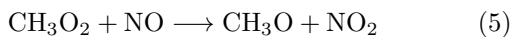
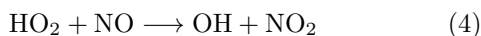
with net:



This is a null cycle for ozone production and destruction, but it determines the NO_x partition in equilibrium with ozone [2]. The photochemical degradation of NO_2 into NO and O depends on a sufficient flux of photons at the appropriate wavelength [3]. During the night, NO_x is present almost exclusively as NO_2 as a result of the reaction (2) above [1]. When steady state of the catalytic cycle is assumed, the O_3 concentration can be predicted as [3]:

$$[O_3]^{ph} = \frac{j_{NO_2}[NO_2]}{k_1[NO]} \quad (3)$$

where the bracket notation defines the concentrations of the respective compounds, j_{NO_2} is the photolysis rate (s^{-1}) in (1) and k_1 is the temperature-dependant rate constant ($ppbv^{-1}s^{-1}$) for the reaction (2) [3]. This is known as the photostationary state for O_3 . The primary source of O_3 in the troposphere is due to the reactions of peroxy radicals (PO_2) with NO [1], such as:



followed by (1). Where HO_2 and CH_3O_2 represent two of many other possible radical groups, depending on the oxidated volatile organic compound (VOC). PO_2 can be either organic (RO_2), or hydro (HO_2) ($[PO_2] = [HO_2] + \sum_i [RO_2]_i$) [3][2]. The reaction of NO with PO_2 driving O_3 production in the troposphere competes with the reaction of NO with O_3 driving the null cycle [1]. Tropospheric destruction of O_3 is due to its reaction with OH and HO_2 (as well as with H_2O through O('D)) and to dry deposition at the surface. However, in the PBL only dry deposition is significant [2]. The net rate of $[O_3]$ can then be defined:

$$\left. \frac{d[O_3]}{dt} \right]_{\text{net}} = k_1[NO][HO_2] + \sum_i k_i[NO][RO_2] \dots \dots - \frac{v_d}{\Delta z}[O_3] \quad (6)$$

where v_d is the dry-deposition velocity at the surface. It is then useful to define the Leighton ratio:

$$\Phi = \frac{[O_3]^{ph}}{[O_3]} = \frac{j_{NO_2}[NO_2]}{k_1[NO][O_3]} \quad (7)$$

where $[O_3]$ represents a measured value of O_3 concentration. The difference at any point between the photostationary state and the measured value, represented either by the relative concentrations themselves or by deviation of the Leighton ratio from unity, is due to the presence of RO_2 of the total value of the peroxy radicals [2], so that:

$$[PO_2] = \frac{j_{NO_2}[NO_2]}{k_1[NO]} - \frac{k_1[O_3]}{k_2} \quad (8)$$

where k_2 is the temperature-dependant rate coefficient for the reaction (4)[3]. The Leighton ratio tends to unity if chemical cycles are faster than transport so that no other reactions (other than of NO and O_3) are able to close the catalytic cycle initiated by the photolysis of NO_2 . Assuming deviation from unity of the Leighton ratio is due solely to the presence of PO_2 , a further generalization-or first order approximation-of the Leighton ratio can be made including NO_x cycles with PO_2 :

$$\Phi_1 = \frac{j_{\text{NO}_2}[\text{NO}_2]}{k_1[\text{NO}][\text{O}_3] + k_2[\text{NO}][\text{PO}_2]} = \frac{\Phi}{1 + \frac{k^*}{k} \frac{[\text{PO}_2]}{[\text{O}_3]}} \quad (9)$$

where k^* is an average of k and $\{k_i\}$.

The Ozone Box Model reviewed here in the following three cases attempts to calculate the present O_3 concentration in three possible modes of complexity. The first and simplest mode the model can use to calculate O_3 concentrations is by using purely dynamical considerations to attribute concentration fluctuations; this means the model uses meteorological data to determine the effective transport of O_3 from the stratosphere and calculate the concentrations in the boundary layer. This mode is implemented by setting the total contribution of chemistry to O_3 concentrations to zero:

$$\left. \frac{d[\text{O}_3]}{dt} \right|_{\text{chem}} = [\text{O}_3]_{\text{chem}} = 0$$

The second mode the model can follow to calculate O_3 concentrations is by indirectly calculating the organic radicals through the knowledge of $[\text{NO}]$ and $[\text{NO}_2]$ [2]. In the presence of sunlight, the photo-dissociation coefficient of NO_2 is greater than zero, allowing the photostationary state of ozone $[\text{O}_3]^{ph}$ to be calculated (3). Comparing this value with the measured value for O_3 (7), the simplified chemistry model indirectly deduces the sum of all the peroxy radicals (8), then the chemical production term is assumed $k^*[\text{NO}][\text{PO}_2]$ [2].

The third mode the model uses is a full chemistry approach, which combines dynamics with direct measurement of radical concentrations in order to calculate O_3 contribution by chemical reaction, the resulting O_3 calculation then results from (6).

2 US Campaigns

In this section, data will be analysed with the box model from two campaigns in the United States. The first takes place at PROPHET forest tower observatory in Pellston, Michigan. This location is characterized by little to no VOC pollution. The second campaign is located in Houston, Texas. Houston serves as a strong contrast to the Pellston campaign, as it is a large city with heavy amounts of pollution. The US campaigns offer complete and accurate measurements of all reactive species, offering a good basis to test the ozone model.

2.1 Pellston

The low concentrations of air pollutants allowed by the remoteness of the Pellston location means that complex chemistry plays a less significant role in modeling O_3 concentrations. The plot of $[\text{O}_3]^{ph}$ calculated values along with measured values (Figure 1) shows a tight correlation between the diurnal cycle of the two, suggesting that the NO_x catalytic cycle is a dominant process in this area. The diurnal cycle of O_3 has a range of approximately 10-80 ppbv.

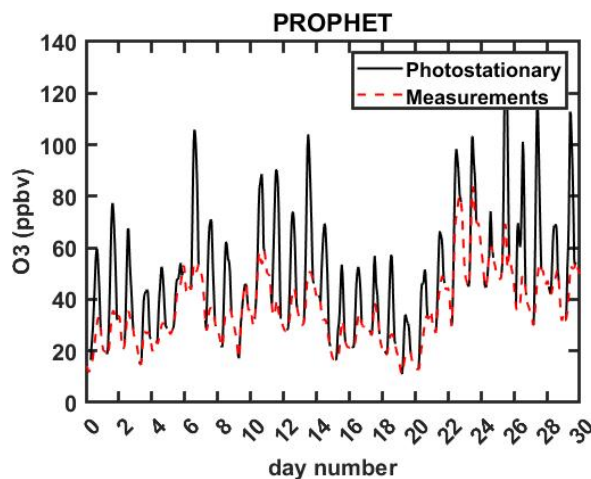


Figure 1: Monthly values for the ozone photostationary state ($[\text{O}_3]^{ph}$) with measured values from the PROPHET site in Pellston, Michigan.

The plot of NO_x concentrations (Figure 2) shows a clear spike in $[\text{NO}]$ correlated with a decrease in $[\text{NO}_2]$ around sunrise, as the photolysis of NO_2 begins, re-initiating the catalytic cycle. However, after sunrise NO concentrations decrease through the day into the night. This is an indication of other chemical processes of NO such as with PO_2 .

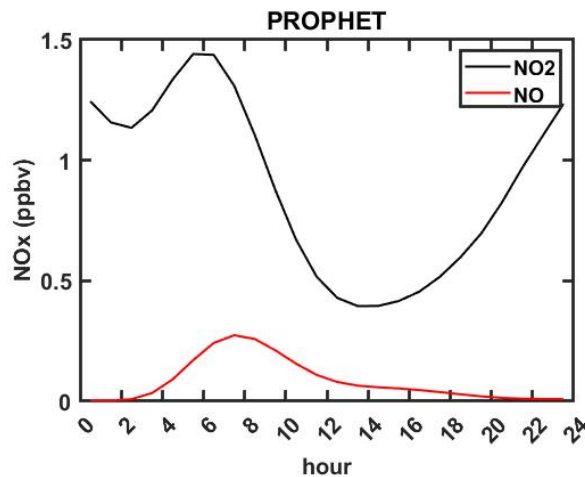


Figure 2: Averaged daily NO_x concentration values from the PROPHET campaign.

The Leighton ratio (Figure 3) allows further analysis of the balance of ongoing chemical processes. The value of Φ deviates positively from unity when some chemical processes are ongoing other than the NO_x catalytic cycle [3]. Φ reaches unity around 6 am correlated with sunrise; however, it continues to rise to midday, where it reaches a maximum of 1.71 before decreasing into the evening. The second order approximation, Φ_1 ranges in value from approximately 0.65 in the morning and evening, with a midday max of approximately 1.19.

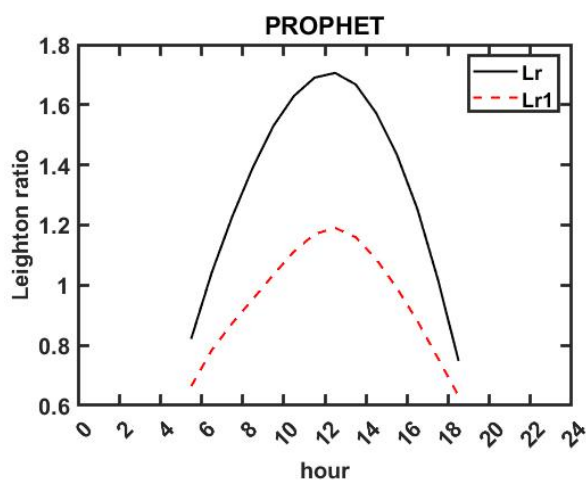


Figure 3: Daily Leighton ratio Φ and first order approximation Φ_1 from the PROPHET site. Values for the Leighton ratio are only available during daytime hours when photolysis initiates the NO_x catalytic cycle and the ozone photostationary state can be calculated.

The Ozone box model performed well under the data from the PROPHET campaign. With full chemistry consideration, the model was able to calculate the O_3 concentrations with a total correlation of 0.9047 between the modelled and measured values, and an average daytime correlation of 0.9315.

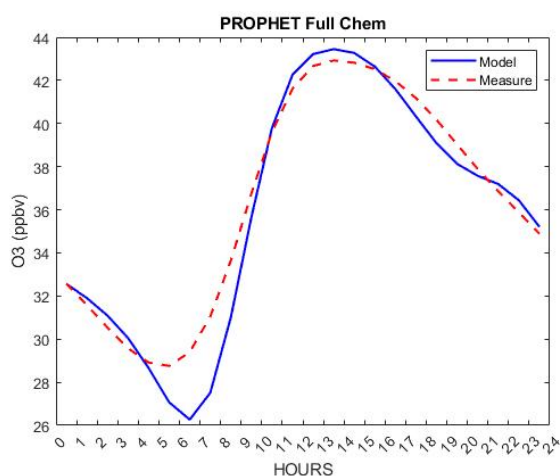


Figure 4: Daily cycle of calculated and measured ozone concentrations for the PROPHET campaign with full chemistry consideration.

The plot (4) of modeled and measured values for O_3 in the PROPHET campaign with full chemistry consideration shows correct modeling of the diurnal cycle, with an under prediction during night times of approximately 2.5-3 ppbv, and a slight over prediction during midday of approximately 0.5 ppbv. With simplified chemistry consideration, the model performed similarly to that of full chemistry, with a total correlation of 0.8984, and a daytime correlation of 0.8635. It's obvious that the simplified chemistry model should perform well during night hours when there are fewer ongoing chemical processes; however, the simplified approach

showed slight shortcomings during daytime hours when it was not able to perfectly calculate all of the ongoing processes, presumably those involving the decrease in NO concentration seen in Figure 2 during daytime hours.

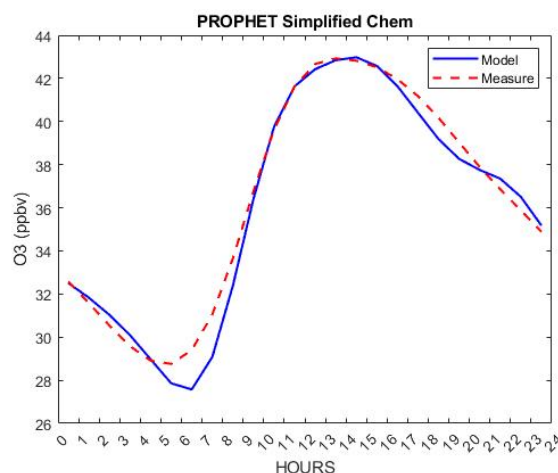


Figure 5: Daily cycle of calculated and measured ozone concentrations for the PROPHET campaign with simplified chemistry consideration.

The plot of modeled and measured O_3 values with simple chemistry consideration (Figure 5) shows the model follows the measure values in the diurnal cycle well. Similar to the full chemistry model, the nighttime values are under predicted; however, the simplified chemistry model appears to more closely follow measured values between late morning into early afternoon. These results are rather ambiguous, as the correlation values indicate the full chemistry model has superior accuracy, and plots indicate the simplified chemistry model is more accurate. If a purely dynamical model is considered, a total correlation of 0.8923 is achieved, with a daytime correlation of 0.9284. This result is surprisingly accurate, and can be attributed once again to the remoteness of the campaign location.

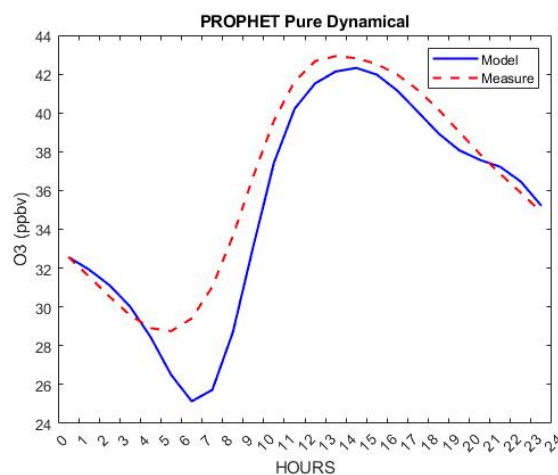


Figure 6: Daily cycle of calculated and measured ozone concentrations for the PROPHET campaign with only dynamical consideration.

The plot of the purely dynamic modeled values for O_3 along with measured values (Figure 6) clearly indicates under representation of O_3 values from early morning and into the evening. This result seems ambiguous as well, as it appears inconsistent with the correlation between the modeled and measured value.

2.2 Houston

A large city such as Houston presents more complexities when attempting to model atmospheric chemistry conditions in comparison to the Pellston location. Larger concentrations of PO_2 and VOCs in conjunction with increased solar flux (lower latitude) means a more diverse spectrum of chemical processes. In addition, Houston is located near the coast of the Gulf of Mexico, adding to the dynamical complexity of the location. This is evident when considering the difference between photostationary and measured values for O_3 (Figure 7). Photostationary values for O_3 range from 10-120 ppbv with an average daily range of approximately 60 ppbv. Measured O_3 values ranged from 1-190 ppbv with an average daily range of approximately 100 ppbv. Discrepancy between measured and photostationary values for O_3 ranged from measured values 30-40 ppbv under photostationary value to measured values 30-60 ppbv over photostationary value. Surprisingly, some days showed measured values adhering closely to photostationary values.

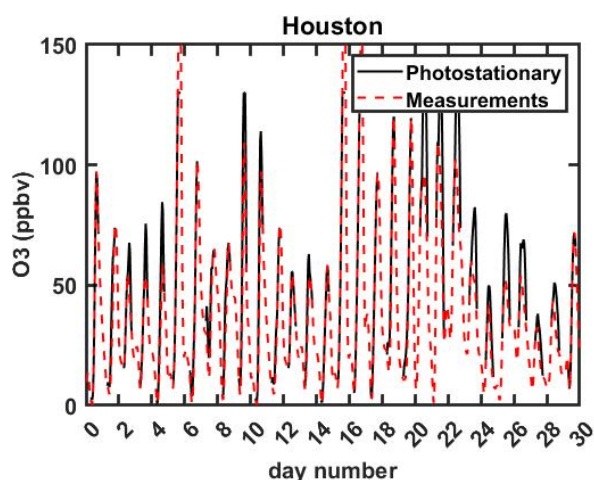


Figure 7: Monthly values for O_3 photostationary state and measured values in Houston, Texas.

Average NO_x values in Houston (Figure 8) were approximately 10-15 times higher than in the Pellston location. NO values increased from a minimum around midnight of 0.1 ppbv to a maximum around 9am of 6.26 ppbv. Average values for NO_2 show two minimums, at midnight and at 1400, with values of 9.26 ppbv and 8.35 ppbv, respectively. NO_2 values increased through the night and peaked just after 6am at approximately 14.21 ppbv.

The Leighton ratio (Figure 9) shows midday values (during photolytic steady states) of 1.299 just after 9am. The values are relatively stable, decreasing only

to 1.279 ppbv by 1430. Values for Φ_1 were consistently less than unity, approaching unity at noon with a value of 0.964, then decreasing.

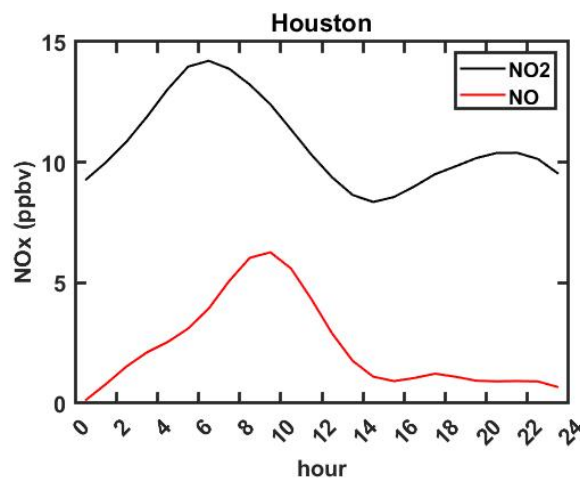


Figure 8: Average daily NO_x concentration values in Houston, Texas. Note that these values are an order of magnitude higher than those in the Pellston location (Figure 2)

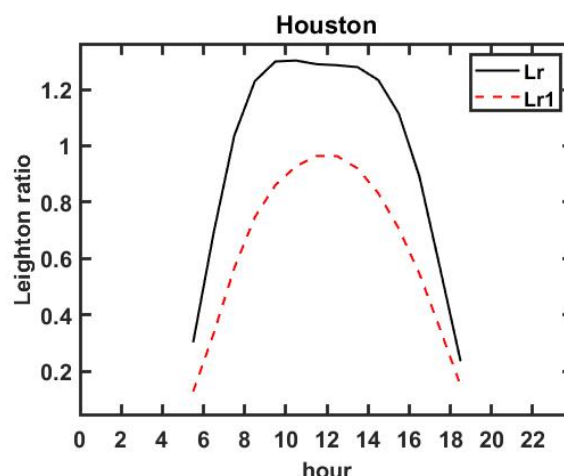
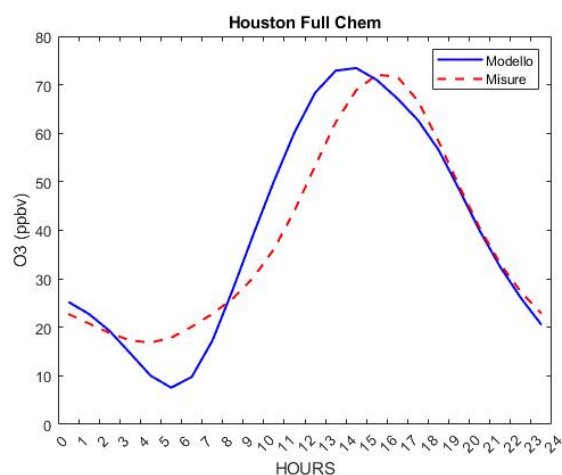
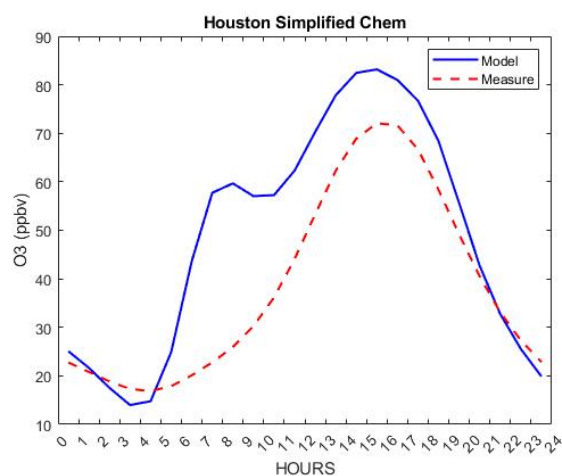


Figure 9: Average daily values for the Leighton ratio Φ and Φ_1 in Houston, Texas. Once again, this can only be calculated during daytime hours following calculation of the ozone photostationary state. It is noteworthy here the similar range to the PROPHET location but with lower min and max values.

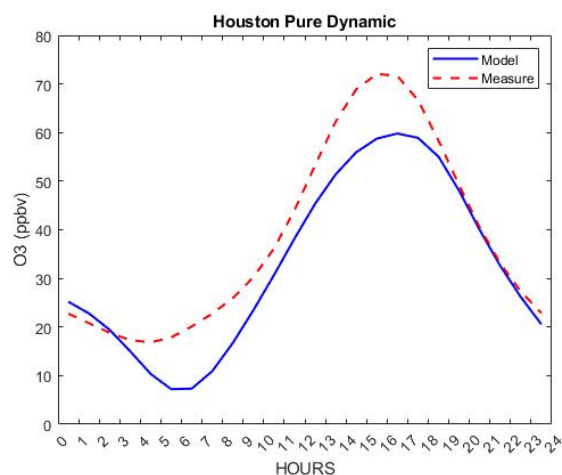
The box model performance at the Houston location was low with respect to the Pellston location. The model with full chemistry consideration achieved a total correlation of 0.5207, with a correlation of 0.3656 during daytime hours. With simplified chemistry, the model achieved a total correlation of 0.5934, with a daytime correlation of 0.4910. With purely dynamic considerations, the model achieved a total correlation of 0.5905, and a daytime correlation of 0.5237. The average diurnal cycle with modelled and measured O_3 values for the three cases are shown in Figure 10.



(a)



(b)



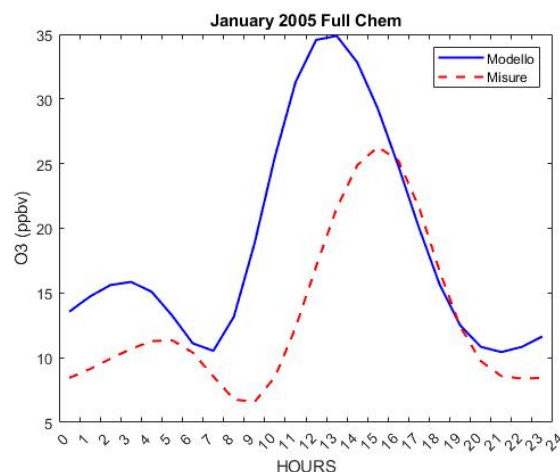
(c)

Figure 10: Average daily modeled and measured values for O_3 with full chemistry (a), simplified chemistry (b) and pure dynamical (c) consideration in Houston, Texas.

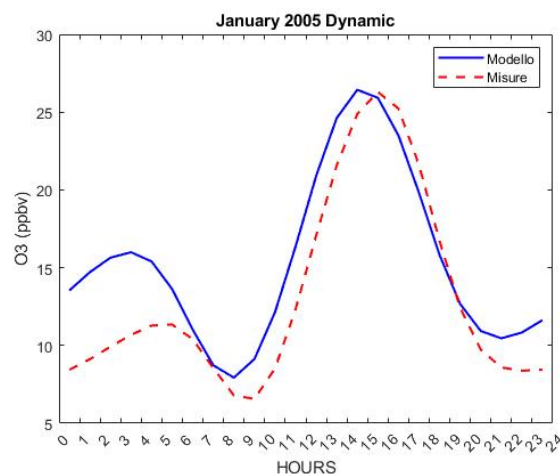
3 L'Aquila

The US campaigns of PROPHET and Houston have been reproduced in L'Aquila, Italy, acquiring data over multiple years. The data was acquired from a station

on the edge of the city; the accuracy of reactive species concentrations taken here was low with respect to the US campaigns. Data was available for 20 months during 2005, 2006 and 2007; the results of the box model are available in Table 1 (Figure 13). At first glance the data reported in Table 1 appears to show a trend of increasing model accuracy by total correlation from winter months into summer months; however, averaging the for each month from different years (Table 2, Figure 14) shows the models performance was relatively consistent throughout the year. Total correlations range from 0.61-0.80 for the full chemistry model and from 0.60-0.79 in the dynamic model in the averaged data. Mixing accounted for approximately 45-50% of the O_3 source with full chemistry consideration, and 48-51% with purely dynamical consideration. Chemistry accounted for a small percentage of the total O_3 production, from only approximately 0.5-1% in the winter months and 3-6.5% in the summer months.



(a)



(b)

Figure 11: Average daily modeled and measured values for O_3 with full chemistry (a) and pure dynamical (b) considerations during January 2005 in L'Aquila.

Figure 11 shows the O_3 diurnal cycle for the modeled and measured values with both full chemistry and purely dynamical consideration in January of 2005; these plots are considerably different despite the models

performance in the two cases showing statistical similarity (Table 1). January 2005 shows the lowest net chemical production of all the months for which data is available, a characteristic expected to increase dynamical model performance. Using the full chemistry, the model appears to over estimate the chemical contribution to morning-time O_3 production, resulting in a midday difference of ~ 10 ppbv.

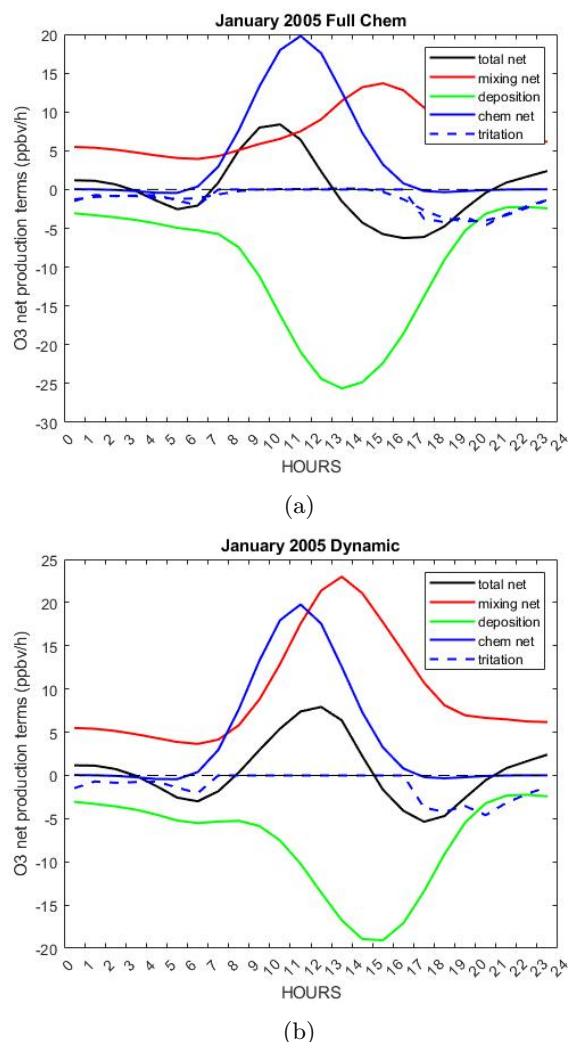


Figure 12: Net O_3 production terms with full chemistry (a) and pure dynamical (b) considerations during January 2005 in L'Aquila.

This is more evident in Figure 12, which shows the diurnal cycle of O_3 net production terms for both full chemistry and dynamic cases. Both dynamic and full chemistry models overestimate nighttime O_3 values (Figure 11), which could result from either overestimation of nighttime mixing, or underestimation of nighttime deposition (Figure 12). The total correlation for January 2005 was 0.4495 with full chemistry consideration and 0.4447 with purely dynamical considerations. This is relatively low performance in comparison to the US campaign performance; however, when averaged with results from January 2007 (a year with higher correlation model performance) the model achieved a correlation of 0.6195 and 0.6166 for full chemistry and purely

dynamical considerations, respectively.

In contrast to results from January, the model performed slightly better in July both with full chemistry and purely dynamics, with a total correlation of 0.7473 and 0.7182, respectively. The O_3 diurnal cycle for the two considerations of July are shown in Figure 15. Both considerations again underestimate peak O_3 concentrations; however, the full chemistry consideration appears to more accurately follow the morning spike in concentration than for January, which may suggest the full chemistry model is more accurate in summer months when chemistry plays a larger role. The dynamic consideration for July 2006 shows the inverse of the full chemistry consideration when compared to January; morning concentration changed are underestimated-again suggesting a chemistry playing a larger role than in January-which continues until the evening. Both full chemistry and dynamical models underestimate max O_3 concentrations by approximately 10 ppbv.

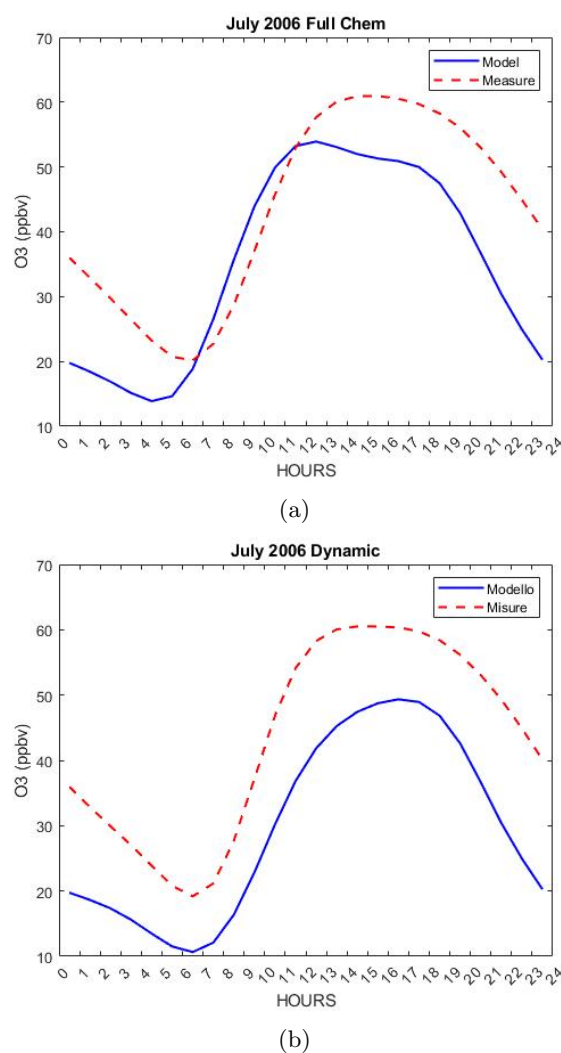
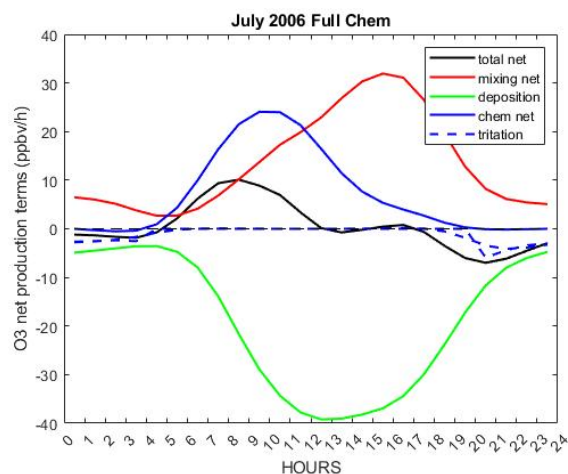


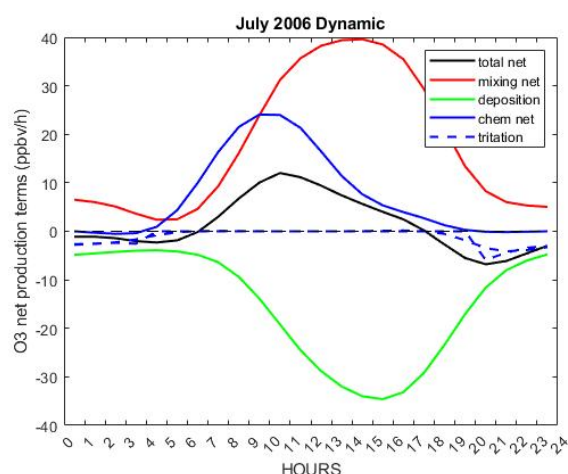
Figure 15: Average daily modeled and measured values for O_3 with full chemistry (a) and pure dynamical (b) considerations for July 2006 in L'Aquila.

The net O_3 production terms for the two cases (Figure 16) show large differences in estimation of both mixing

and deposition contribution, similar to case in January months, with ~ 10 ppbv higher midday deposition estimation in the full chem model, and ~ 10 ppbv higher midday mixing production in the dynamic model. Unlike the January run, the July run estimates slightly more net chemistry contribution (~ 5 ppbv) with the full chemistry model.



(a)



(b)

Figure 16: Net O_3 production terms with full chemistry (a) and pure dynamical (b) considerations during July 2006.

4 Conclusion

The ozone box model performed quite differently in each of the three scenarios above; however, it performs considerably well in unpolluted sites when paired with accurate measurements of reactive agents. The best result came from all three modes of the model at the PROPHET location, with the full chemistry consideration achieving a total correlation of 0.9047. The box model performed less accurately with the L'Aquila data for all months available, with max total correlations reaching just over 0.80 with full chemistry consideration, and purely dynamical consideration just under at 0.79. The model had the lowest performance in the Houston campaign, with total correlation for the three

modes ranging 0.52-0.59. From the performance of the model in the three locations it is possible to conclude that model performance is directly dependant upon the complexity of both the chemistry and dynamics of the location. The model performs best with full chemistry consideration, but is very capable of recovering contributions from peroxy radicals through the simplified chemistry approach, and therefor serves as an excellent tool for analysis of chemical reactant contributions in relatively unpolluted locations.

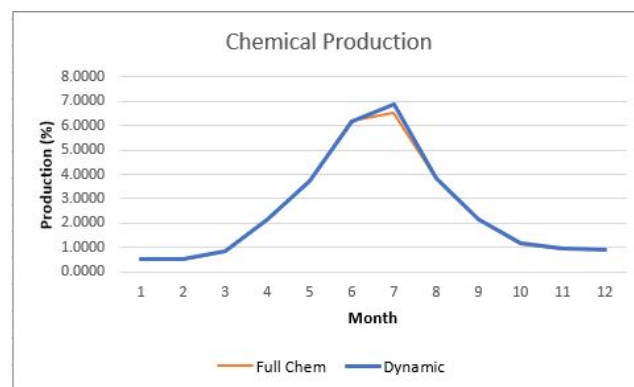


Figure 17: From Table 2: Yearly cycle for chemical ozone production with full chemistry and purely dynamical consideration.

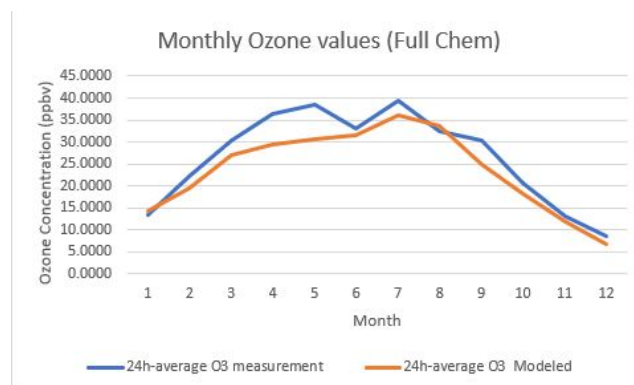


Figure 18: From Table 2: Yearly cycle for average ozone concentrations with full chemistry consideration.

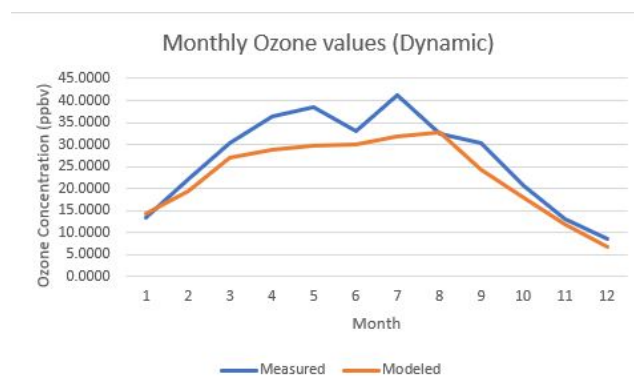


Figure 19: From Table 2: Yearly cycle for average ozone concentrations with purely dynamical consideration.

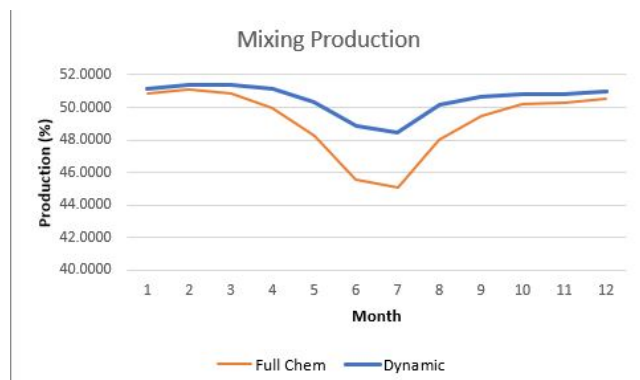


Figure 20: From Table 2: Yearly cycle for mixing ozone production with full chemistry and purely dynamical consideration.

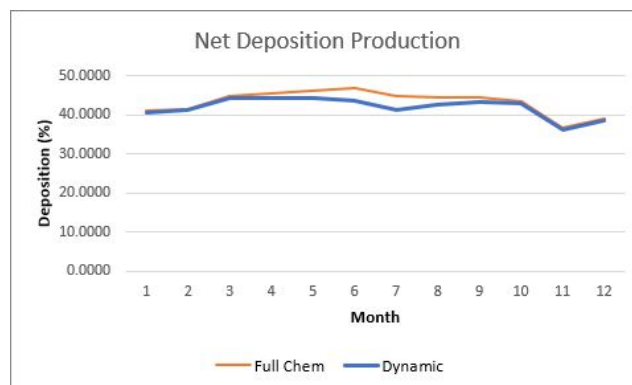


Figure 23: From Table 2: Yearly cycle for ozone deposition with full chemistry and purely dynamical consideration.

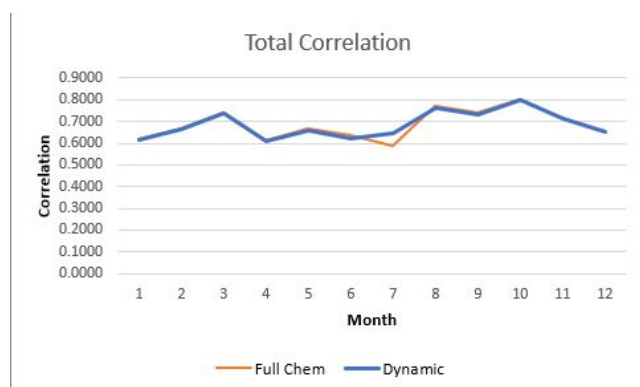


Figure 21: From Table 2: Yearly cycle for correlation between modeled and measured ozone values with full chemistry and purely dynamical consideration.

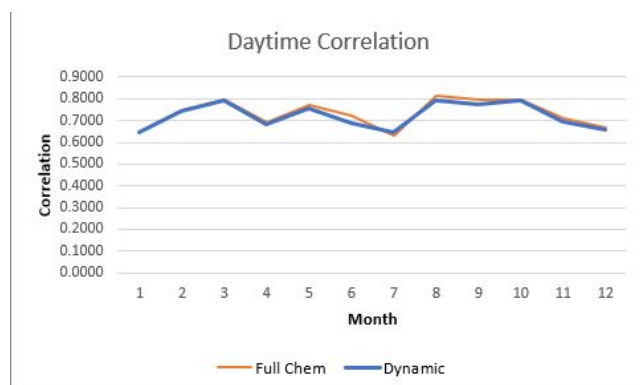


Figure 22: From Table 2: Yearly cycle for daytime correlation between modeled and measured ozone values with full chemistry and purely dynamical consideration.

References

- [1] Daniel J. Jacob. 11. *Oxidizing Power of the Troposphere*, pages 200–230. Princeton University Press, 1999.
- [2] Giovanni Pitari. Lecture notes from environmental meteorology, November 2021.
- [3] Robert J. Griffin, Pieter J. Beckman, Robert W. Talbot, Barkley C. Sive, and Ruth K. Varner. Deviations from ozone photostationary state during the international consortium for atmospheric research on transport and transformation 2004 campaign: Use of measurements and photochemical modeling to assess potential causes. *Journal of Geophysical Research: Atmospheres*, 112(D10), 2007.

Month	Year	chem	Total Correlation	Daytime Correlation	Net Mixing Production (%)	Net Deposition Production (%)	Net Titration Production (%)	Net Chemical Production (%)	24h-average O ₃ measurement	24h-average O ₃ Modeled
Janaury	2005	FULL	0.4495	0.5419	51.0146	41.7480	6.8299	0.4075	13.1185	15.3756
February	2005	FULL	0.6831	0.7368	51.0761	43.5021	4.9636	0.4581	24.9893	21.0322
March	2005	FULL	0.7624	0.7940	50.8491	45.5682	2.9212	0.6614	30.6641	29.1032
April	2005	FULL	0.7262	0.7214	50.1998	45.5630	2.5750	1.6622	36.6690	32.4960
May	2005	FULL	0.7323	0.8323	49.8780	46.8788	1.2608	1.9824	33.8595	33.1711
June	2005	FULL	0.7540	0.7552	46.4641	46.9508	1.3204	5.2647	31.4165	31.3878
July	2005	FULL	0.5889	0.6290	45.0760	44.8994	3.5154	6.5093	39.4210	35.9458
August	2005	FULL	0.7393	0.8259	47.9349	44.2463	4.0327	3.7862	27.4899	32.6562
July	2006	FULL	0.7473	0.7684	44.1762	45.2702	3.1248	7.4289	43.2555	31.2844
August	2006	FULL	0.8005	0.8069	48.1095	45.1373	2.7620	3.9912	37.5696	34.3781
September	2006	FULL	0.7410	0.7949	49.4943	44.4146	3.9221	2.1689	30.3965	24.7854
October	2006	FULL	0.8005	0.7974	50.1988	43.5355	5.0951	1.1707	20.5711	18.1398
November	2006	FULL	0.7169	0.7076	50.2676	36.7808	12.0163	0.9353	13.0167	11.8896
December	2006	FULL	0.6578	0.6704	50.5129	39.1680	9.3917	0.9275	8.6890	6.6753
Janaury	2007	FULL	0.7897	0.7582	50.6244	40.3322	8.3832	0.6602	13.8780	13.2731
February	2007	FULL	0.6478	0.7512	51.1863	39.5225	8.7013	0.5900	19.1967	17.9520
March	2007	FULL	0.7215	0.7965	50.9340	44.0888	3.9561	1.0212	29.6933	25.1509
April	2007	FULL	0.4988	0.6683	49.7460	45.3787	2.2395	2.6358	36.1810	26.1998
May	2007	FULL	0.5996	0.7089	46.6609	45.6653	2.2025	5.4713	43.1218	27.8272
June	2007	FULL	0.5175	0.6953	44.5742	46.6639	1.5934	7.1685	34.5494	31.4555
Janaury	2005	NONE	0.4447	0.5358	51.2260	41.5404	6.8259	0.4076	13.1185	15.3218
February	2005	NONE	0.6821	0.7355	51.3245	43.2593	4.9581	0.4581	24.9893	20.9539
March	2005	NONE	0.7610	0.7933	51.2135	45.2104	2.9150	0.6611	30.6641	28.9734
April	2005	NONE	0.7206	0.7093	51.0722	44.7127	2.5585	1.6566	36.6690	32.1650
May	2005	NONE	0.7294	0.8250	50.9619	45.8150	1.2485	1.9745	33.8595	32.7654
June	2005	NONE	0.7468	0.7351	49.2905	44.2081	1.2817	5.2197	31.4165	30.2133
July	2005	NONE	0.5711	0.5760	48.6084	41.5580	3.4280	6.4057	39.4210	34.4000
August	2005	NONE	0.7305	0.7997	49.9767	42.3039	3.9684	3.7510	27.4899	31.8640
July	2006	NONE	0.7182	0.7127	48.2276	41.4122	3.0312	7.3291	43.2555	29.5294
August	2006	NONE	0.7879	0.7849	50.2890	43.0504	2.7141	3.9465	37.5696	33.5233
September	2006	NONE	0.7310	0.7765	50.6848	43.2410	3.9056	2.1687	30.3965	24.3576
October	2006	NONE	0.7965	0.7908	50.8342	42.9109	5.0827	1.1722	20.5711	17.9451
November	2006	NONE	0.7103	0.6947	50.8073	36.2717	11.9852	0.9357	13.0167	11.7706
December	2006	NONE	0.6526	0.6600	50.9991	38.7053	9.3676	0.9280	8.6890	6.6087
Janaury	2007	NONE	0.7886	0.7546	50.9876	39.9916	8.3607	0.6602	13.8780	13.1992
February	2007	NONE	0.6457	0.7464	51.5049	39.2160	8.6890	0.5901	19.1967	17.8567
March	2007	NONE	0.7197	0.7923	51.4901	43.5482	3.9419	1.0198	29.6933	24.9692
April	2007	NONE	0.4935	0.6571	51.1629	43.9918	2.2203	2.6250	36.1810	25.7362
May	2007	NONE	0.5890	0.6849	49.6354	42.7568	2.1673	5.4405	43.1218	26.6849
June	2007	NONE	0.4955	0.6412	48.3803	42.9982	1.5280	7.0935	34.5494	29.9018

Figure 13: (Table 1) Correlation values with production terms and averaged O₃ values for each month with both full chemistry and pure dynamical consideration.

Month	chem	Total Correlation	Daytime Correlation	Net Mixing Production (%)	Net Deposition Production (%)	Net Titration Production (%)	Net Chemical Production (%)	24h-average O ₃ measurement	24h-average O ₃ Modeled
Janaury	FULL	0.6196	0.6500	50.8195	41.0401	7.6066	0.5338	13.4983	14.3243
February	FULL	0.6654	0.7440	51.1312	41.5123	6.8324	0.5240	22.0930	19.4921
March	FULL	0.7420	0.7952	50.8916	44.8285	3.4386	0.8413	30.1787	27.1271
April	FULL	0.6125	0.6949	49.9729	45.4708	2.4073	2.1490	36.4250	29.3479
May	FULL	0.6659	0.7706	48.2695	46.2721	1.7316	3.7268	38.4907	30.4992
June	FULL	0.6358	0.7252	45.5192	46.8073	1.4569	6.2166	32.9830	31.4216
July	FULL	0.5889	0.6290	45.0760	44.8994	3.5154	6.5093	39.4210	35.9458
August	FULL	0.7699	0.8164	48.0222	44.6918	3.3973	3.8887	32.5298	33.5171
September	FULL	0.7410	0.7949	49.4943	44.4146	3.9221	2.1689	30.3965	24.7854
October	FULL	0.8005	0.7974	50.1988	43.5355	5.0951	1.1707	20.5711	18.1398
November	FULL	0.7169	0.7076	50.2676	36.7808	12.0163	0.9353	13.0167	11.8896
December	FULL	0.6578	0.6704	50.5129	39.1680	9.3917	0.9275	8.6890	6.6753
Janaury	NO	0.6166	0.6452	51.1068	40.7660	7.5933	0.5339	13.4983	14.2605
February	NO	0.6639	0.7409	51.4147	41.2376	6.8235	0.5241	22.0930	19.4053
March	NO	0.7404	0.7928	51.3518	44.3793	3.4285	0.8405	30.1787	26.9713
April	NO	0.6071	0.6832	51.1176	44.3523	2.3894	2.1408	36.4250	28.9506
May	NO	0.6592	0.7549	50.2987	44.2859	1.7079	3.7075	38.4907	29.7251
June	NO	0.6211	0.6882	48.8354	43.6031	1.4049	6.1566	32.9830	30.0575
July	NO	0.6447	0.6444	48.4180	41.4851	3.2296	6.8674	41.3382	31.9647
August	NO	0.7592	0.7923	50.1328	42.6772	3.3413	3.8488	32.5298	32.6936
September	NO	0.7310	0.7765	50.6848	43.2410	3.9056	2.1687	30.3965	24.3576
October	NO	0.7965	0.7908	50.8342	42.9109	5.0827	1.1722	20.5711	17.9451
November	NO	0.7103	0.6947	50.8073	36.2717	11.9852	0.9357	13.0167	11.7706
December	NO	0.6526	0.6600	50.9991	38.7053	9.3676	0.9280	8.6890	6.6087

Figure 14: (Table 2) Averaged values from Table 1 for months with data for more than one year.